Ongoing over-exploitation and delayed responses to environmental change highlight the urgency for action to promote vertebrate recoveries by 2030: Supplementary Material

Richard Cornford[1,2,3,†] (ORCID: 0000-0002-9963-3603),
Fiona Spooner[4] (ORCID: 0000-0001-6640-8621),
Louise McRae[1] (ORCID: 0000-0003-1076-0874),
Andy Purvis[2] (ORCID: 0000-0002-8609-6204),
Robin Freeman[1]

1: Institute of Zoology, Zoological Society of London, London, NW1 4RY, UK
2: Department of Life Sciences, Natural History Museum, London, SW7 5BD, UK
3: Department of Life Sciences, Imperial College London, Berkshire, SL5 7PY, UK
4: Our World in Data at the Global Change Data Lab, Oxford, OX2 0DP, UK
† Present address: IIASA, International Institute for Applied Systems Analysis (IIASA), Biodiversity and Natural Resources Program, 2361 Laxenburg, Austria

S1 Supplementary analysis

S1.1 Year- versus generation-based lags

In our preliminary analysis, we considered both year-, and generation-based lags for our models. Having found little evidence that generation-based lags were better (Fig S1.1) we settled on using year-based lags in the remainder of the main analyses for clarity and consistency across vertebrate groups.

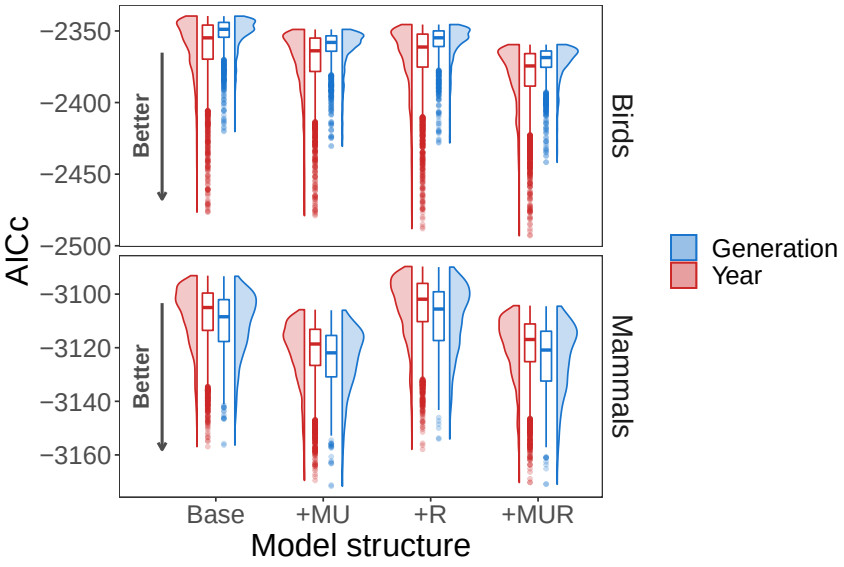

Figure S1.1: **Across the range of model structures tested, we did not find overwhelming support in favour of either year-, or generation-based lags.**
In preliminary analysis, we considered both year-, and generation-based lags. Whilst most bird models are improved by year-based lags, the case is less clear for mammals. We therefore settled on using year-based lags in the remainder of the main analyses for clarity and consistency across vertebrate groups.
Boxplots depict the 25%, 50% and 75% quantiles. Whiskers extend 1.5x the interquartile range from the upper/lower quartiles. Points indicate outliers.
Base models incorporate climate change, land-use change (and their interaction), body mass and protected area status as fixed effects. +MU models additionally incorporate management and utilisation status. +R models are as the Base models, but also including realm. +MUR represents models incorporating all of the above variables as fixed effects.

S1.2 Influential populations

As shown in Table S1.1, the best year-based models we initially identified where strongly influenced by certain populations and/or species (Cook's D > 0.5). We therefore removed these data points and re-applied the model fitting and lag selection methodology to obtain the results presented in the main text. Investigation of the best +MU models (those we use in the main text) indicates no further strong influence of certain species/populations (Cook's D < 0.5 and coefficients stable under cross-validation, Fig S1.2). Data without the influential populations was also used when conducting all analysis presented below.

Table S1.1: **Summary of populations/species that were found to strongly influence the best models in our initial analysis.**

Class	Model	Population/Species	Cook's D
Aves	Base	*Gyps bengalensis*	1.90
	Base	*Podiceps nigricollis*	0.84
	+MU	*Gyps bengalensis*	1.27
	+MU	*Podiceps nigricollis*	0.59
	+R	*Gyps bengalensis*	1.49
	+MUR	*Gyps bengalensis*	1.16
Mammalia	Base	single population of spp. 68	1.02
	Base	all populations of spp. 68	1.02
	+MU	single population of spp. 68	0.63
	+MU	all populations of spp. 68	0.64
	+R	single population of spp. 68	0.60
	+R	all populations of spp. 68	0.63

Due to their substantial influence (Cook's D > 0.5), we removed these bird species and the single population of spp. 68 (which appeared to be driving the above influence) from the data (Note; spp. 68 is used as the population/species in question is confidential within the LPD). We then re-implemented our methods, generating the results presented in the main text.

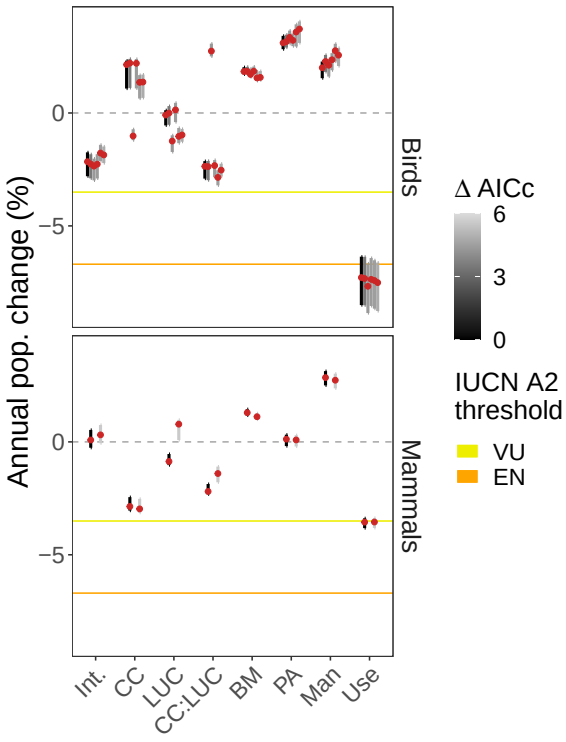

Figure S1.2: **When conducting leave-one-out (population) cross-validation of the top +MU models, coefficients remain consistent.**
Although some variation in coefficient estimates is apparent, especially for the impact of use on birds, the direction and magnitude recorded across cross-validation folds is largely comparable to the results from the full data. Additional analysis also found no populations/species had an undue influence on the models (all Cook's D < 0.5).
Bars represent the range of coefficient values obtained from cross-validation whilst red points indicate the coefficient estimate obtained from the original/full data.
IUCN thresholds correspond to red list threat categories based on population declines of 30% (VU; vulnerable) and 50% (EN; endangered) over 10 years.

S1.3 Including Realm effects highlights geographic differences in abundance trends

In our main analysis, we focus on models without any effect of (biogeographic) Realm. However, for both vertebrate groups, models incorporating Realm-specific intercepts (+MUR) also perform strongly in terms of AICc (Fig S2.17). These models identify similar optimal lags to those in the main analysis (Fig S1.3a), supporting the importance of ecological lags in biodiversity models. Furthermore, the coefficients of the top +MUR models are largely equivalent to those in the +MU models, but additionally emphasise the different biodiversity trends that are occurring in different biogeographic realms (Fig S1.3b), reflecting the complex nature of biodiversity change in the Anthropocene (Blowes et al., 2019; Leung et al., 2020).

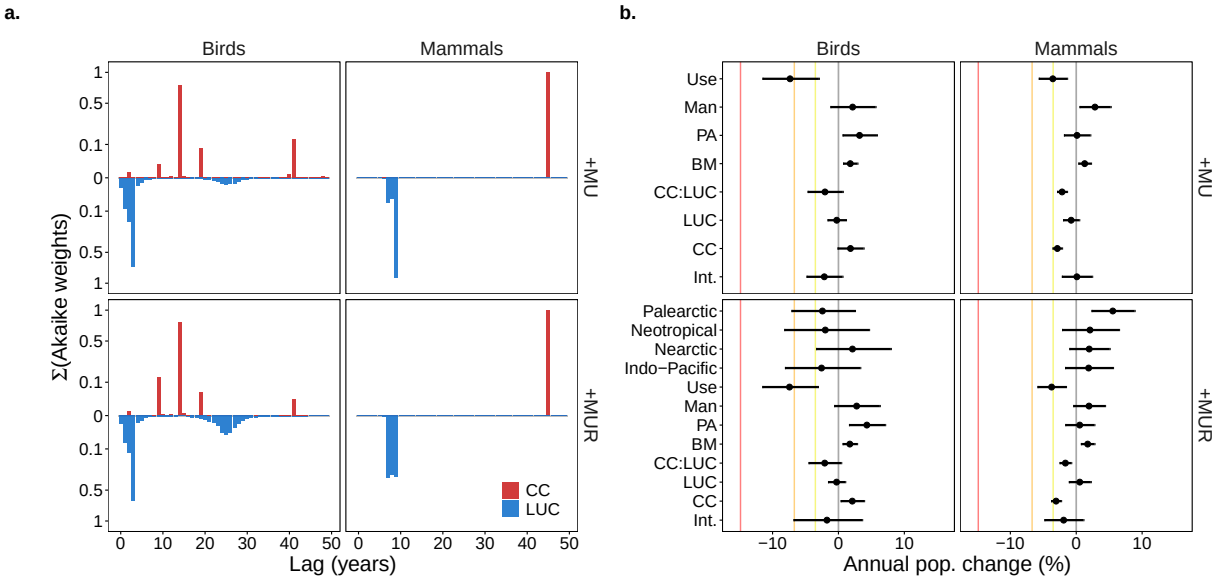

Figure S1.3: **Optimal lags remain highly similar across model structures (a.), and models incorporating realm effects (+MUR) highlight the divergence in average abundance trends across biogeographic realms (b.).**
a. We find optimal lags remain highly similar across the +MU and +MUR models, typically seeing longer optimal lags associated with climate warming (CC) than land-use change (LUC).
b. In both model structures, we find a complex effect of environmental change on vertebrate populations (CC:LUC term). Biological resource use (Use) is consistently the driver with the most negative impact for each class, whereas management and protected areas (for birds) benefit population trends. The inclusion of realm-specific intercepts shows how average population trends differ across space reflecting the complex nature of biodiversity change in the Anthropocene (Blowes et al., 2019; Leung et al., 2020). We find more negative trends for birds in the Indo-Pacific, Neotropics and Palearctic, whereas for mammals, Palearctic populations are doing better than Afrotropical (Int.) ones.
In **b.**, coloured lines correspond to IUCN red list threat categories based on population declines of 30% (yellow; Vulnerable), 50% (orange; Endangered), or 80% (red; Critically endangered) over 10 years (A2 criteria).
In **b.**, the intercept (Int.) of +MUR models includes the effect associated with populations being in the Afrotropical realm. The other realm-related effects are in relation to this (Afrotropical) intercept.

S1.4 Removing short population time-series

Inclusion criteria for population time-series from the LPD were broad, but similar to those in recent work (Spooner, Pearson, & Freeman, 2018; Williams, Freeman, Spooner, & Newbold, 2021). To test the sensitivity of our results to the removal of short time-series, which can often display extreme trends (Leung et al., 2020), we investigated the impact of raising the minimum number of data points per time series (DP min) from 3 to 4, and 5 for models with the +MU structure. When doing so, we find lags (Fig S1.4a) and coefficients (Fig S1.4b) remain consistent for mammals. In birds, the optimal lag associated with climate change increases from 14 to 40 years (Fig S1.4a) whilst the land-use lags, and most coefficients remain similar (Fig S1.4a,b). Interestingly, the delayed effects of land-use become more negative for birds when short time-series are excluded, whilst the individual impact of climate warming (also for birds) appears to become slightly more positive.
This sensitivity analysis reinforces the importance of lagged effects of environmental change on population trends, and further supports the estimated effects of drivers and mitigation approaches.

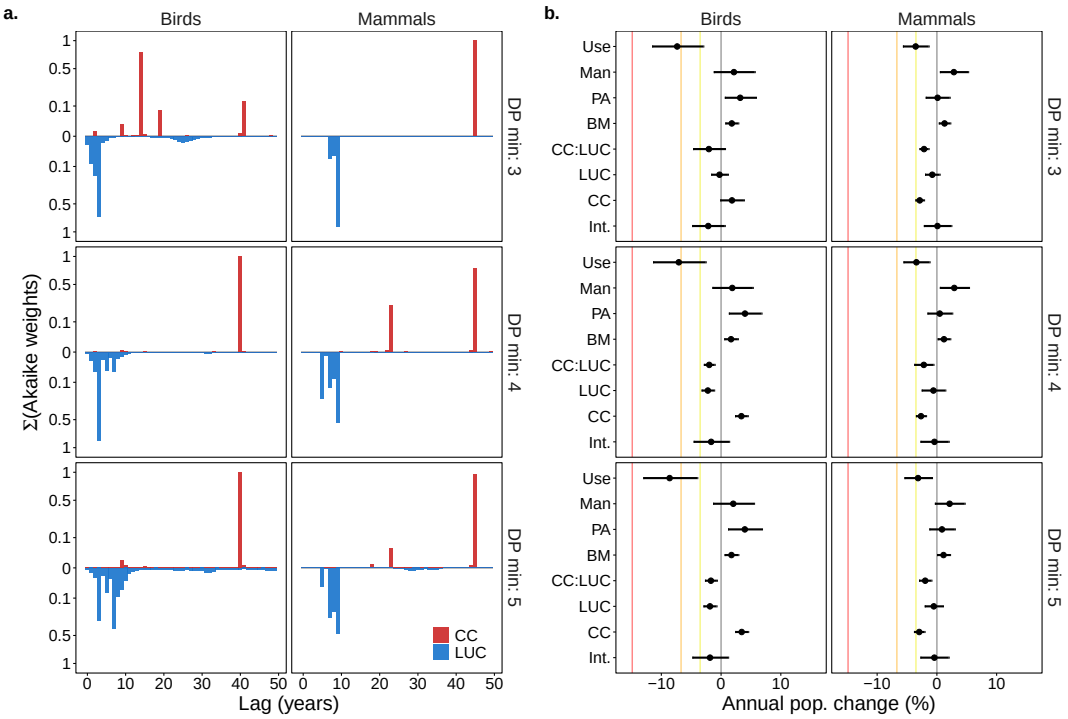

Figure S1.4: **Support for ecological lags (a.) and model averaged coefficients (b.) when considering alternative data point thresholds for population time-series inclusion.**
a. Increasing the inclusion threshold for minimum number of data points per time-series (DP min) has little impact on optimal mammal lags but is associated with longer climate lags for birds.
b. Model-averaged coefficients remain fairly consistent across DP min thresholds.
CC = climate change; LUC = land-use change.
DP min of 3 corresponds to our main analysis.
In **b.**, coloured lines correspond to IUCN red list threat categories based on population declines of 30% (yellow; Vulnerable), 50% (orange; Endangered), or 80% (red; Critically endangered) over 10 years (A2 criteria).

S1.5 Additional ecological subsetting of population data

In addition to the body mass subsetting presented in the main results, we also divided our mammal and bird populations based on trophic level (herbivore or carnivore) and latitude (temperate or tropical), before re-assessing the optimal lags and model coefficients for each subset. We did this to further assess whether the population trends of different ecological subsets are best explained using different lags, e.g., herbivores may respond to land conversion faster than carnivores due to being lower in the food chain. Here, we present results based on the +MU model specification (i.e., incorporating management and biological resource use, but not realm).

It is hard to pick out clear patterns in the optimal lags identified for different data subsets. In mammals, we find that carnivores display longer lags for land-use change than herbivores, but the reverse is true when considering climate warming (Fig S1.5a). Additionally, tropical mammals appear to respond more quickly to warming than temperate counterparts, but we do not find this for birds. Overall, the lags inferred from our complete mammal data appear to be driven by temperate herbivores, whilst the lags found in the main bird analysis are relatively consistent with those found for carnivorous species (Fig S1.5a).

When looking at the coefficients of the optimal models there is some suggestion that tropical/carnivorous mammals benefit most from management whereas temperate/carnivorous birds are most affected by direct exploitation (Fig S1.5b). Surprisingly, these results also suggest that carnivorous mammals decline more when inside a protected area than outside, indicating that further analysis is required to properly verify any identified patterns.

As in our main results, we again find that the estimated effects of climate and land-use change vary substantially depending on the lags considered (Fig S1.5c, showing coefficients from models where both climate and land-use have the same lag). In contrast, the effects of Use (negative), Management (positive) and PAs (positive for birds) remain more consistent across lags and data subsets.

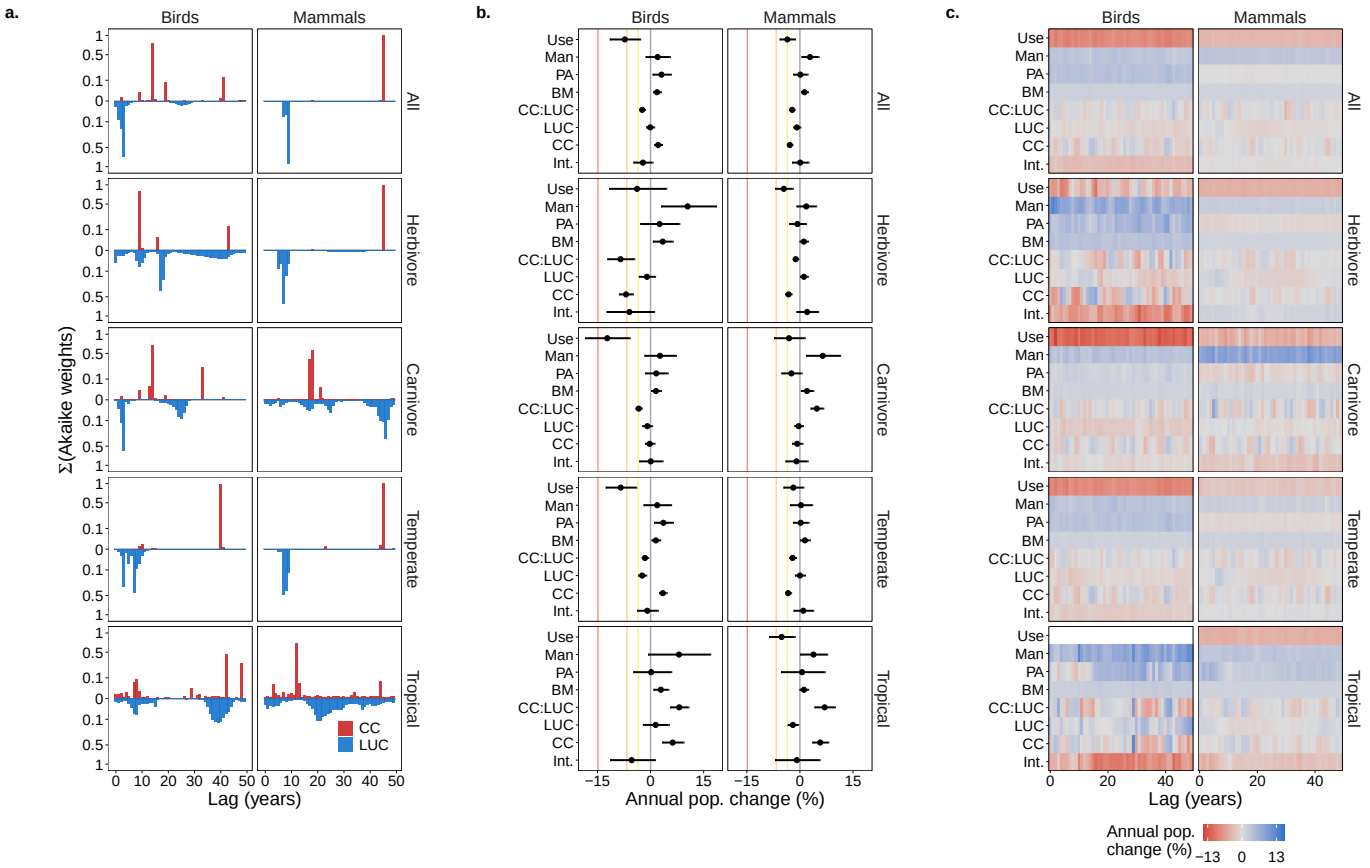

Figure S1.5: **Optimal lags and model coefficients differ amongst ecological subsets, but no over-arching patterns appear to be present.**

Herbivores = diets contain at least 2/3 plants; Carnivore = diets contain at least 2/3 animals; Temperate populations = above 23.5 N or below -23.5 S; Tropical populations = below 23.5 N and above -23.5 S.

CC = climate change; LUC = land-use change.

In **a.**, summed Akaike weights depict a measure of relative support for a particular lag. They are presented on a square root scale to enhance visualisation of lags with relatively low support.

In **b.**, coloured lines correspond to IUCN red list threat categories based on population declines of 30% (yellow; Vulnerable), 50% (orange; Endangered), or 80% (red; Critically endangered) over 10 years (A2 criteria).

S1.6 Categorising interactive effects

We defined the interactions between climate and land-use change following Piggott, Townsend, and Matthaei (2015). Specifically, using models with ΔAICc < 6 we predicted population responses to scaled rates of climate change (annual rate of temperature change) and land-use change (annual rate of change in agricultural land) i) using the main effects only (additive only), and ii) including the climate:land-use interaction term (additive plus interaction). We averaged these predictions over models using Akaike weights to get model averaged predictions. By comparing these predicted responses (i.e., additive only v. additive plus interaction), we assigned synergistic v. antagonistic interactions based on Piggott et al. (2015) (see their Fig 2, and also shown in Côté, Darling, & Brown, 2016, Fig 1).

Figs S1.6 and S1.7 show the model-predicted response to environmental change (a), and the type of interaction between climate and land-use change across this environmental space (b). Whilst much of the prediction space indicates synergistic interactions between the temperature and land-use change variables, there is also some evidence for antagonism (e.g., Fig S1.6 large birds and Fig S1.7 herbivorous mammals).

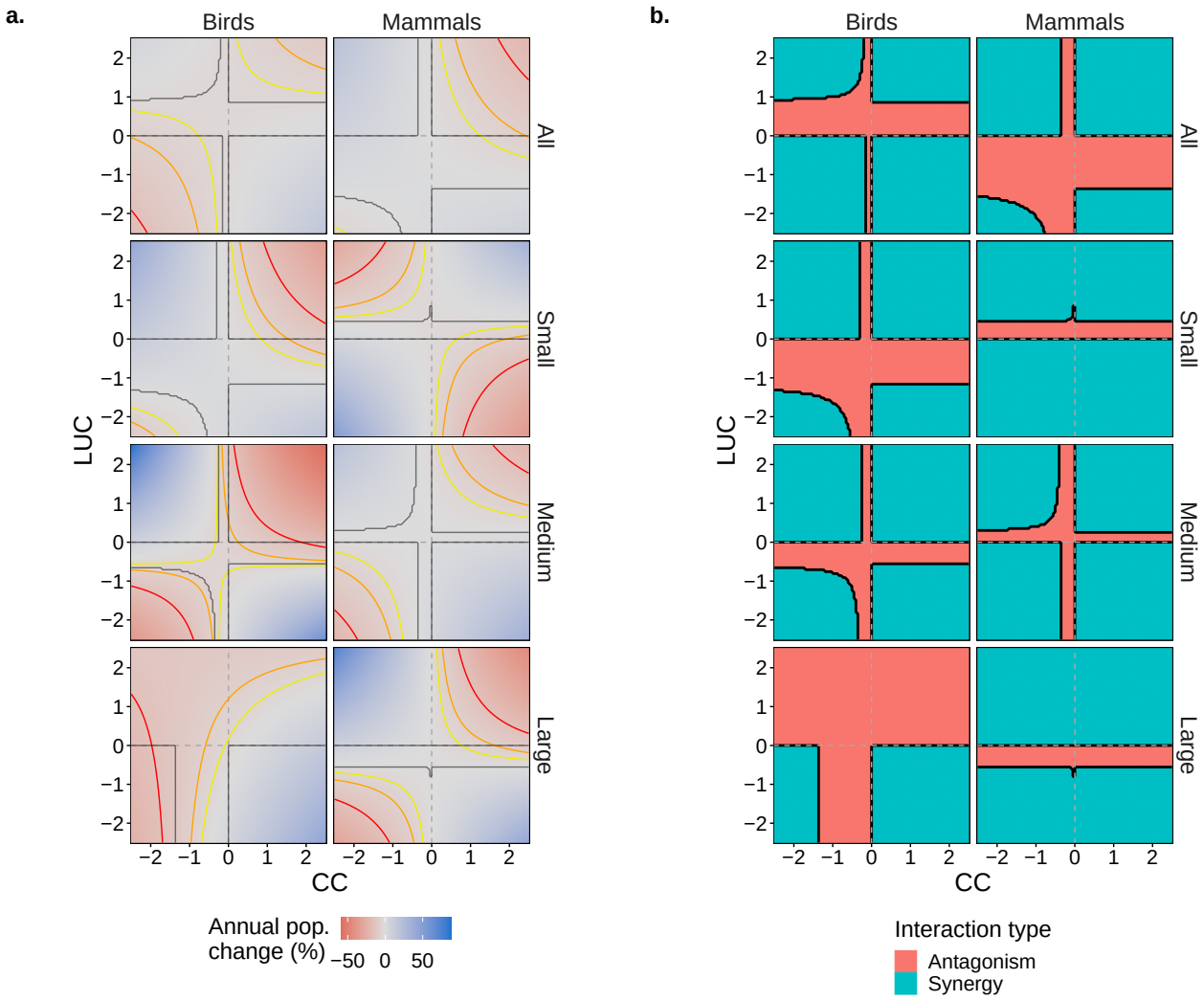

Figure S1.6: **Synergy v Antagonism: Data split based on body mass tertiles.**
a. Predicted average annual rate of population change based on average annual rates of climate warming and land conversion.
b. Classification of the interaction between climate and land-use change, based on environmental change rates, predicted population responses (with/without environmental interaction term) and Piggott et al. (2015).
In **a.**, coloured lines correspond to IUCN red list threat categories based on population declines of 30% (yellow; Vulnerable), 50% (orange; Endangered), or 80% (red; Critically endangered) over 10 years (A2 criteria).
In **a.**, the dark grey lines indicates the boundary between the regions of synergy and antagonism shown in **b**.

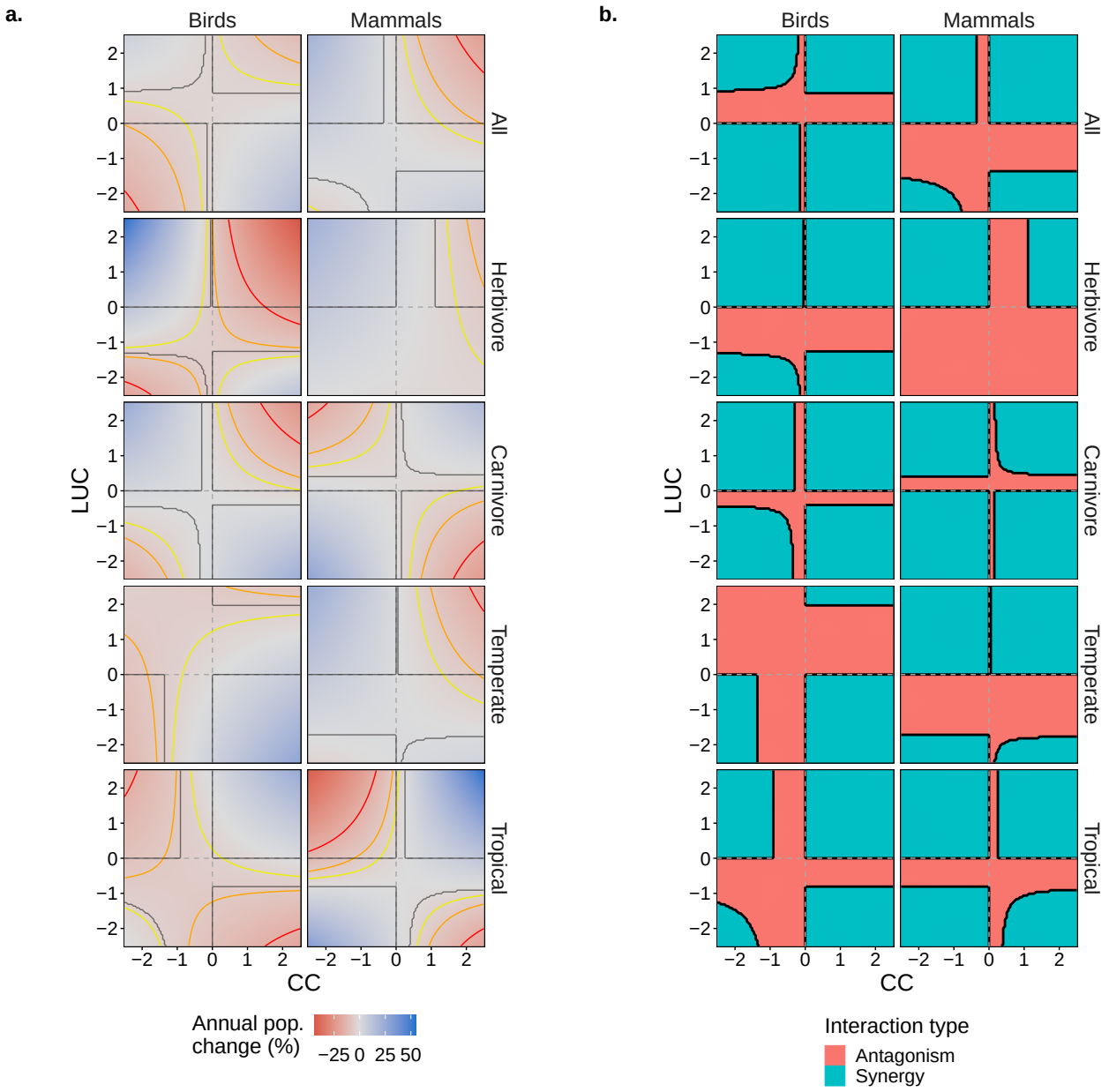

Figure S1.7: **Synergy v Antagonism: Data split based on trophic level and latitude.**
a. Predicted average annual rate of population change based on average annual rates of climate warming and land conversion.
b. Classification of the interaction between climate and land-use change, based on environmental change rates, predicted population responses (with/without environmental interaction term) and Piggott et al. (2015).
In **a.**, coloured lines correspond to IUCN red list threat categories based on population declines of 30% (yellow; Vulnerable), 50% (orange; Endangered), or 80% (red; Critically endangered) over 10 years (A2 criteria).
In **a.**, the dark grey lines indicates the boundary between the regions of synergy and antagonism shown in **b**.

S1.7 Sensitivity to environmental data sources

There are a number of global, gridded temperature and land-use datasets. We therefore assessed the sensitivity of our analysis to using different environmental data sources. In addition to the IPSL and LUH2 datasets used in our main analysis, we considered CRU 4.04 (temperature; Harris, Osborn, Jones, & Lister, 2020) and HYDE 3.2 (land-use; Klein Goldewijk, Beusen, Doelman, & Stehfest, 2017).

Using CRU, we extracted average annual temperatures for each 0.5° grid cell containing any of the modelled populations. Following Spooner et al. (2018) we extracted the percentage cover of anthropogenic land use in the nine 0.083° HYDE grid cells surrounding each population location (the combined size of the nine cells is approx. 0.25°, as in the LUH2 data). We considered anthropogenic land as either i) cropland plus pasture plus converted rangeland, or ii) cropland plus pasture plus all rangeland (incl. rangeland with natural vegetaion). HYDE-based anthropogenic land cover (of either type) was then averaged over the nine cells per location and timepoint. Although post-2000 HYDE data is annual, prior to the year 2000, HYDE data has a decadal temporal resolution. To obtain annual anthropogenic land cover values for each site between 1901–2000 we used linear interpolation with the respective decadal data (Spooner et al., 2018). As in our main analysis we used temperature and land cover data spanning 1901–2014. Rates of environmental change were calculated as described in the main text, with this sensitivity analysis focussing on year-based lags, models with the +MU structure and the inclusion of all populations (except thosw identified as being overly influential).

As shown in Fig S1.8a, the optimal lags associated with environmental change remain fairly consistent for birds, irrespective of the environmental data sets used. Climate lags are approximately 10–20 years, whilst lags due to land-use change are shorter, < 5 years. When considering mammals, much greater variation in optimal lags is seen. Whilst climate lags based on IPSL data are approximately 45 years, lags shorten to just three years when using the CRU dataset. Different optimal lags are also apparent for mammalian responses to land conversion.

Investigating the coefficients of the optimal models across environmental data combinations identifies different relationships between environmental change and population responses (Fig S1.8b). For example, coefficients for climate change shift between positive and negative in both classes, as does the CC:LUC interaction term for birds. These results further highlight the complexity associated with deriving the effects of environmental change on biodiversity. However, we also find that the effects of body mass (BM), protected areas (PA), management (Man) and exploitation (Use) remain consistent across the use of different environmental data. Whilst these covariates are not lag-dependent, the consistency of their effects across models, lags and environmental data further indicates the robustness of their detected impacts.

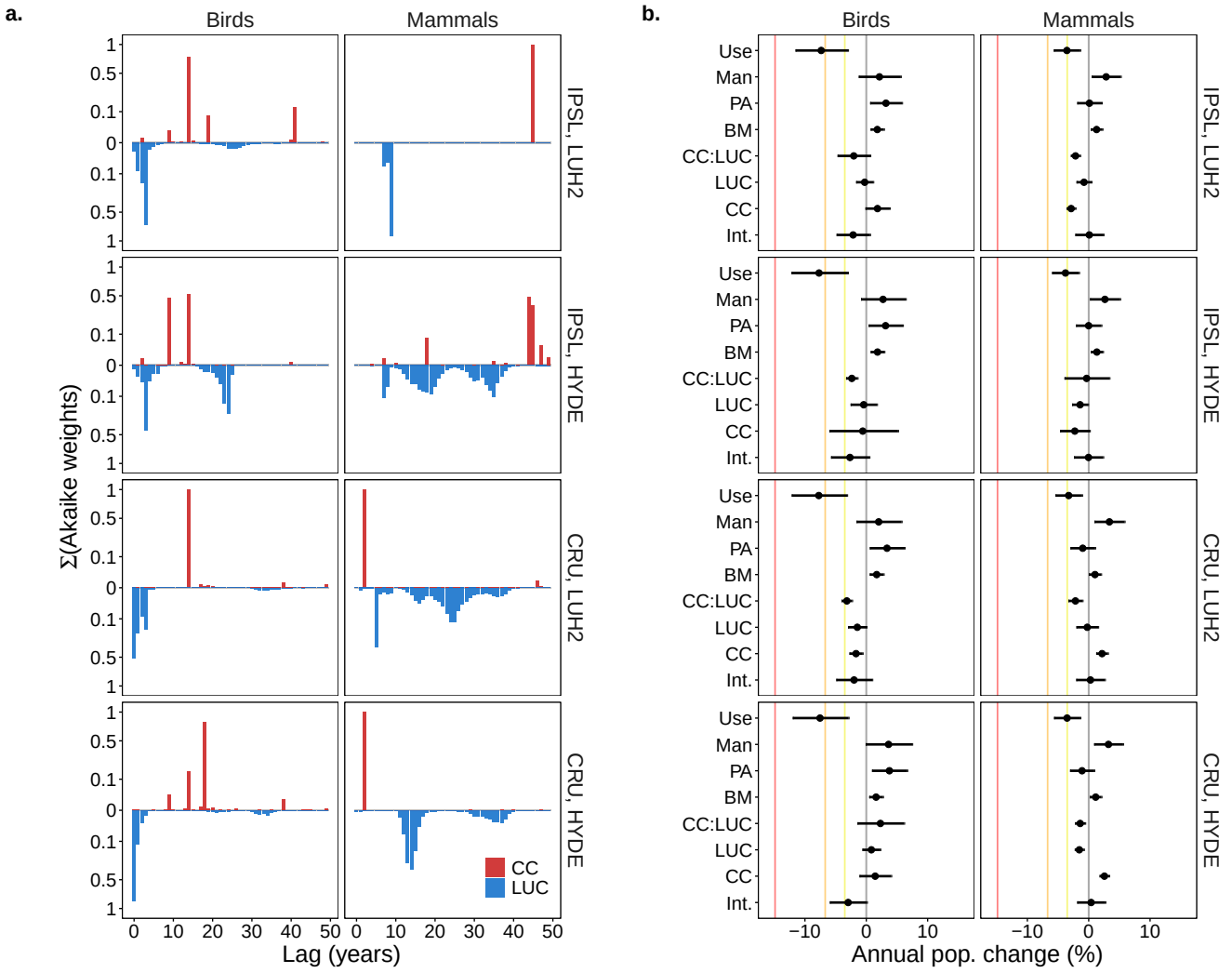

Figure S1.8: **Optimal lags (a.) and coefficient estimates (b.) differ depending on the environmental datasets used.**
CC = climate change; LUC = land-use change.
In **b.**, coloured lines correspond to IUCN red list threat categories based on population declines of 30% (yellow; Vulnerable), 50% (orange; Endangered), or 80% (red; Critically endangered) over 10 years (A2 criteria).
IPSL, LUH2 corresponds to our main analysis.

S1.8 Comparing land-use datasets: rule-based hindcasting v. recent satellite data

Both the LUH2 and HYDE datasets are generated using rule-based land-use allocation algorithms that hindcast from a reference map (recent satellite data is used to inform this reference map, as is FAO data) (Klein Goldewijk et al., 2017). To further evaluate the potential sensitivity of our analysis to alternative land-use data sources, we also compare land-use change in LUH2 to HYDE, and to land-cover changes based on the satellite-derived ESA data (ESA, 2017).

For 1992–2014 (the time period covered by all datasets), we extracted land-use/land-cover data from LUH2, HYDE and ESA for all population locations at a 0.25° resolution. The extraction approach for LUH2 is described in the main text, and for HYDE in Supplementary Material: Sensitivity to environmental data sources (above). For the ESA data, we re-classified the 300m grid cells to cropland (land-cover values 10–40) or not cropland (all other land-cover values), and resampled the dataset to a 0.25° resolution (to match the LUH2 and HYDE data) using bilinear interpolation (Hijmans, 2020). The processed ESA data thus contained average cropland cover per 0.25° per year. We then extracted the grid cells relevant to the modelled population locations. For each unique location (664), and each land-use data source, we estimated annual average change in land-use/land-cover using the mean of annual differences between 1992 and 2014. We assessed the correlation in anthropogenic land-use change estimated at each site between the LUH2 and HYDE data using the slope of a linear model. We compared estimated anthropogenic land-use change in LUH2 to cropland change in ESA using the same approach.

We found significant positive relationships between LUH2- and HYDE-based measures of anthropogenic land-use change (Fig S1.9). In contrast, we found no significant relationship between the LUH2-based measures of land-use change and the ESA-based cropland cover change (Fig S1.10). These results highlight the possibility that, due to discrepancies in land-use/-cover data obtained from alternative sources, ecological models built upon different data sources could differ in their outputs, and subsequent biological inference.

In this work we used land-use (LUH2) and climate (IPSL) data of moderate spatial resolution and extensive temporal extent to evaluate the influence of ecological lags on population abundance trends. Although the use of data with finer spatial resolution (e.g., ESA) would be preferable, such data would not facilitate a thorough analysis of delayed environmental impacts due to restrictive temporal coverage (the ESA start year of 1992 is after the start of many LPD time-series). We therefore prioritised the use of extensive temporal coverage over finer spatial resolution to explore a wider range of possible lags.

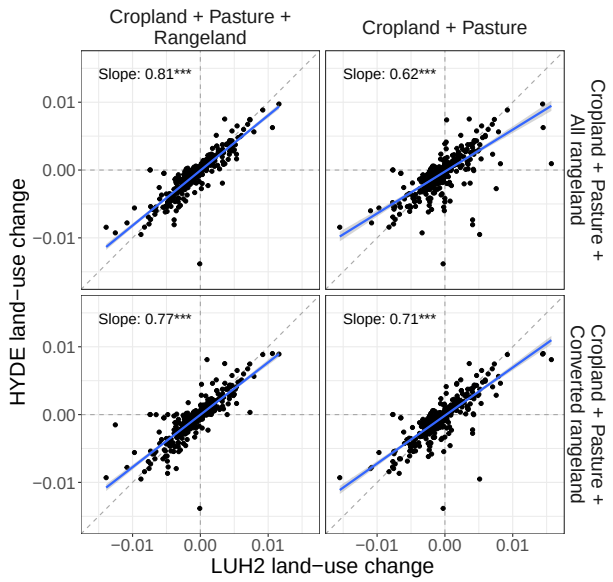

Figure S1.9: **Comparison of anthropogenic land-use change estimates using the LUH2 or HYDE datasets.**
Strong, positive relationships between land-use change estimates derived from either LUH2 or HYDE are apparent.
***: $p < 0.001$, significance of slope in linear model.
Column headings indicate form of LUH2-based anthropogenic land-use, row headings indicate form of HYDE-based anthropogenic land-use.
Each point represents a single location associated with a population in our main analysis.

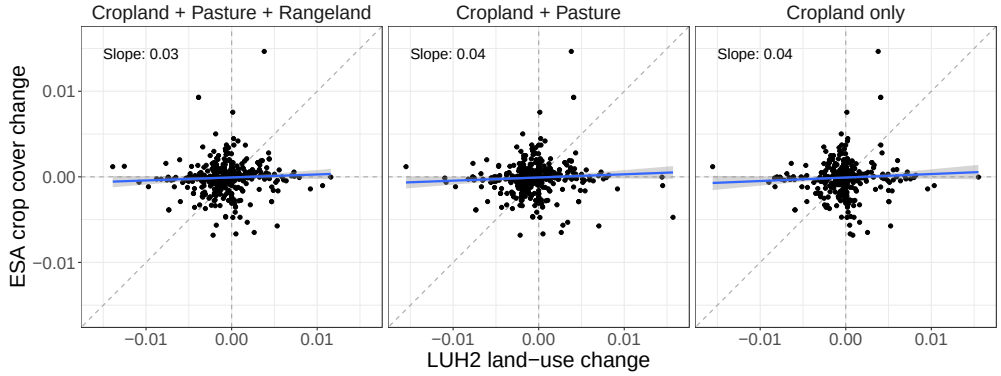

Figure S1.10: **Comparison of anthropogenic land-use/cover change estimates using the LUH2 or ESA datasets.**
We do not find evidence for a positive relationship between land-use change estimates derived from LUH2 and ESA, even if considering only cropland in LUH2 (right panel).
Column headings indicate form of LUH2-based anthropogenic land-use.
Each point represents a single location associated with a population in our main analysis.

S1.9 Model checks

We performed standard model checks on our best models from our main results (ΔAICc = 0, including all populations), evaluating the normality of residuals and testing for spatial, phylogenetic and temporal auto-correlation.

Normality of residuals

Using the `performance` package (Lüdecke, Ben-Shachar, Patil, Waggoner, & Makowski, 2021), we found that model residuals display slightly heavy tails (Figs S1.11c and S1.12c). We tested the use of an inverse hyperbolic sine (IHS) transformation of our response variable (Burbidge, Magee, & Robb, 1988) but found it did not improve the model diagnostic plots (Figs S1.11a,c,e v S1.11b,d,f, and Figs S1.12a,c,e v S1.12b,d,f) Although not perfect, such heavy tails typically lead to wider parameter confidence intervals/standard errors, thus we expect our model output to be conservative.

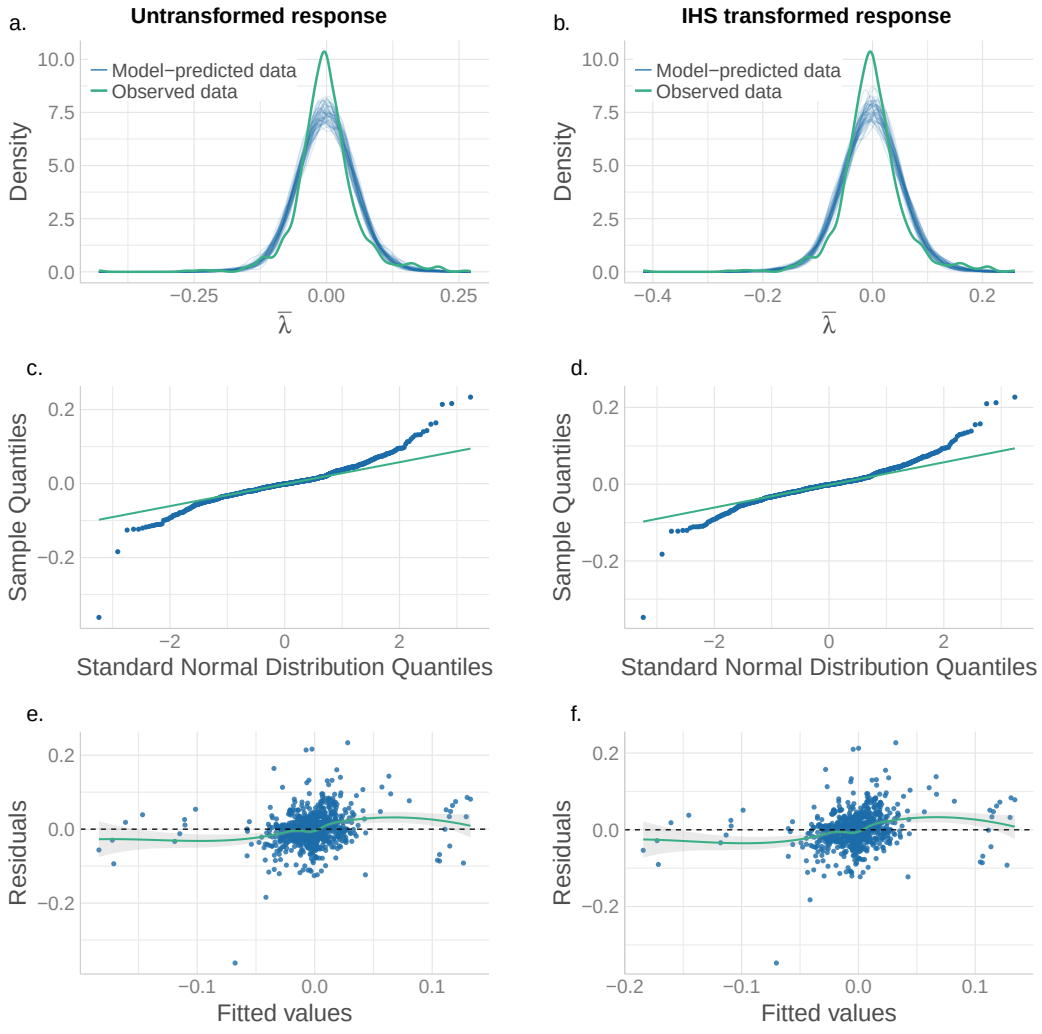

Figure S1.11: **Bird model checks**
Although our model residuals demonstrate slight departure from normality (a, c, e), using an IHS transformation provides no clear benefit (b, d, f).

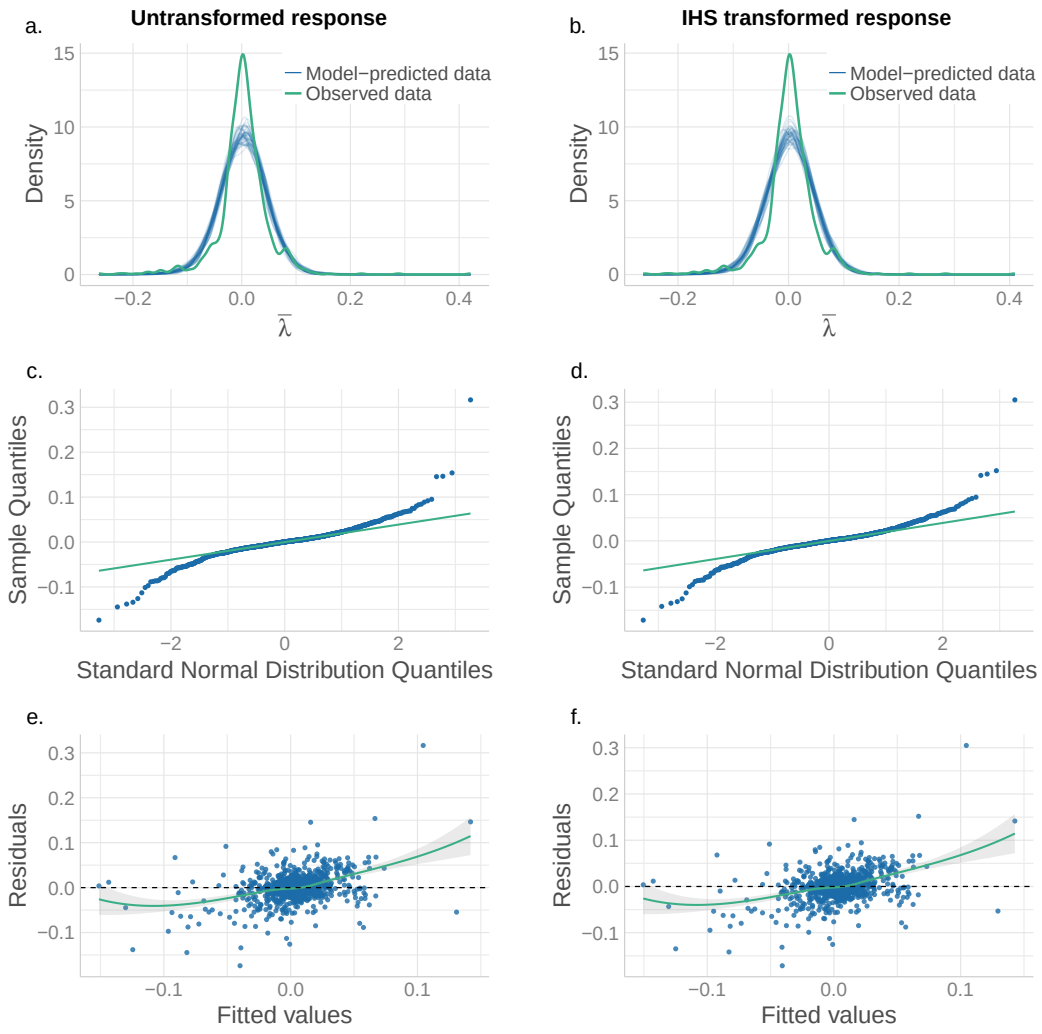

Figure S1.12: **Mammal model checks**
Although our model residuals demonstrate slight departure from normality (a, c, e), using an IHS transformation provides no clear benefit (b, d, f).

Spatial auto-correlation

We checked for spatial auto-correlation in model residuals using a two-tailed Moran's I test (Paradis & Schliep, 2019). Our distance matrix contained the inverse of geographic distance (in metres) (Hijmans, 2021) between population locations, with weights on the diagonal set to 0. We found Moran's I to be significantly more negative than expected for both birds (I = -0.048, $p < 0.05$) and mammals (I = -0.081, $p < 0.001$). The negative Moran's I suggest the residual error in our models is more dispersed (checker-board like) than the null expectation, possibly due to over-compensation within the location random effect. We experimented with including an additional 'Country' random effect (with location nested within this), but found that this had little impact on Moran's I (Birds: I = -0.045, $p < 0.05$; Mammals: I = -0.076, $p < 0.001$). We therefore retained our original random effects structure.

Phylogenetic auto-correlation

To assess for potential phylogenetic auto-correlation in model residuals we used Pagel's lambda (Revell, 2012) and phylogenetic trees from Open Tree of Life (Michonneau, Brown, & Winter, 2016; OpenTreeOfLife et al., 2019). We found no evidence for phylogenetic auto-correlation (Fig S1.13; Birds: $\lambda = 0.03$,

p = 0.17; Mammals: $\lambda = 0.00007$, p = 1).

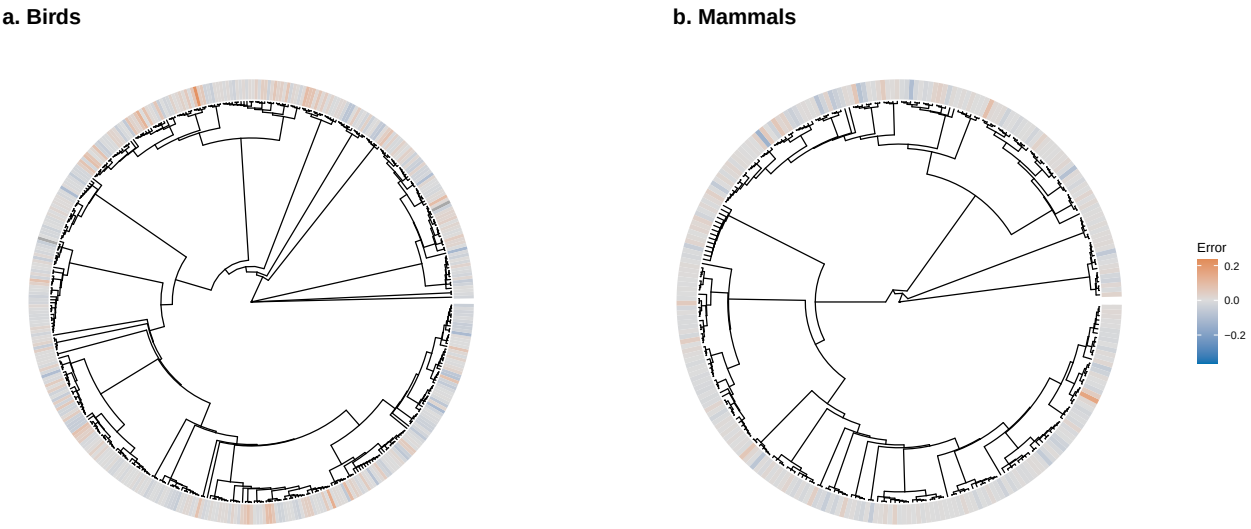

Figure S1.13: **Residual model error in relation to phylogenetic relationships.**
Using Pagel's λ we found no evidence for phylogenetic autocorrelation in our model residuals.
Mammals: $\lambda = 0.00007$, p = 1; Birds: $\lambda = 0.03$, p = 0.17)
Error is the average error per species. Species trees were sourced from the Open Tree of Life.

Temporal auto-correlation

We plotted residual error in response to time-series start date, finding no temporal patterns (Fig S1.14a). Additionally, we fitted a linear model linking average error associated with start year t (explanatory) to average error in start year $t+1$ (response). Again, we found no evidence for temporal auto-correlation in our model residuals (Fig S1.14b; Birds: slope = 0.064, p = 0.663; Mammals: slope = 0.005, p = 0.738).

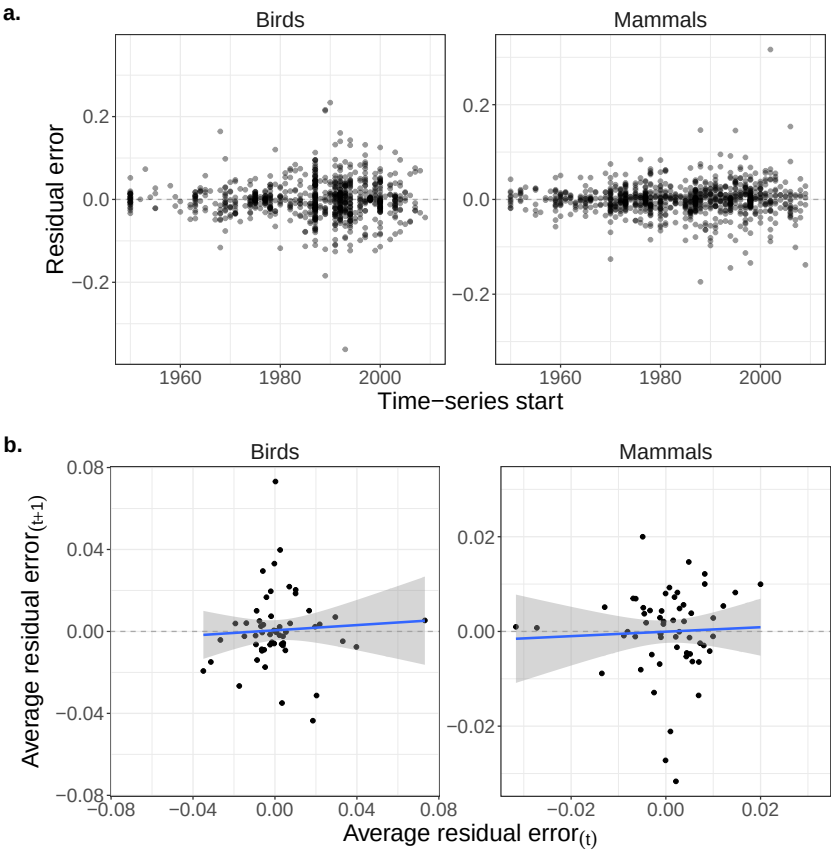

Figure S1.14: **Residual model error in relation to the start year of each population time-series.**
a. A plot of error against time-series start year indicates no clear temporal pattern.
b. A linear model of average residual error in start year t+1 in response to average residual error in start year t reveals no significant relationship.
Birds: slope = 0.064, p = 0.663; Mammals: slope = 0.005, p = 0.738

S2 Supplementary figures

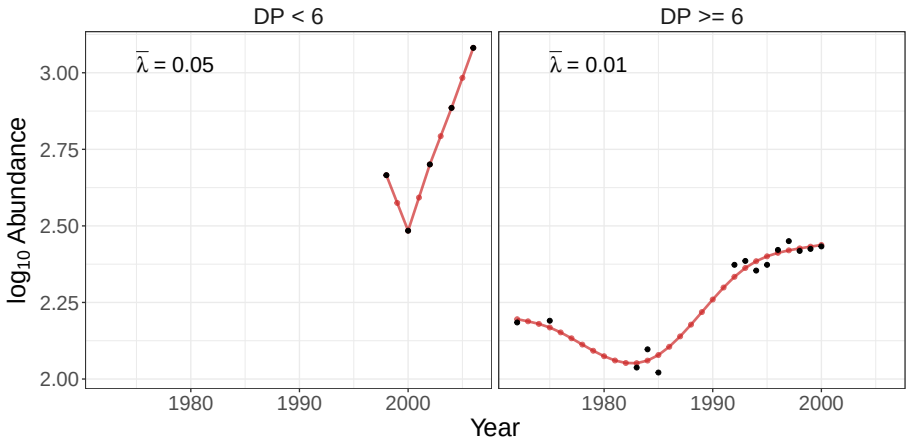

Figure S2.15: **Graphical depiction of our approach to estimating population trends ($\bar{\lambda}$).** When population time-series have fewer than six data points (DP < 6) we used $\log_{10}$-linear interpolation to get abundance values for the missing years. For time-series with at least six data points (DP $>= 6$) we used a generalised additive model to predict abundance values per year across the monitoring period.

A population's average logged rate of annual change ($\bar{\lambda}$) was calculated as: $\bar{\lambda} = \frac{\sum_{t=2}^{T} log_{10}(\frac{N_t}{N_{t-1}})}{T-1}$, where T is the total number of years in the interpolated time-series and N_t is the abundance value in year t (Spooner et al., 2018).

Black points show recorded population abundance values.

Red points and lines show model inferred abundance values.

Data on the left are from a Hippo (*Hippopotamus amphibius*) population, data on the right are from a Lemur (*Lemur catta*) population.

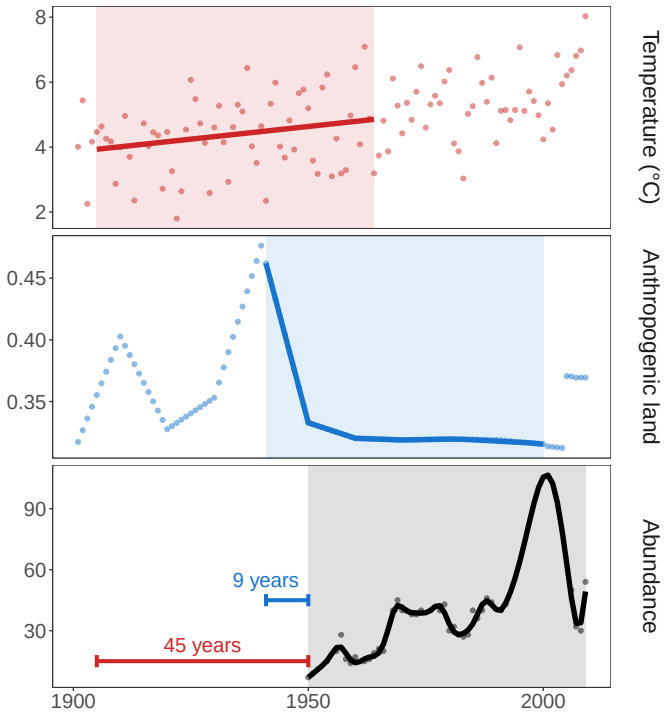

Figure S2.16: **Graphical depiction of our approach to assigning lagged environmental change to population time-series.**
Here, the lag associated with climate warming is 45 years, and 9 years for land conversion, matching the results from our main Mammal model.
Graphics are illustrative and based on data from a managed beaver (*Castor fiber*) population in Russia.

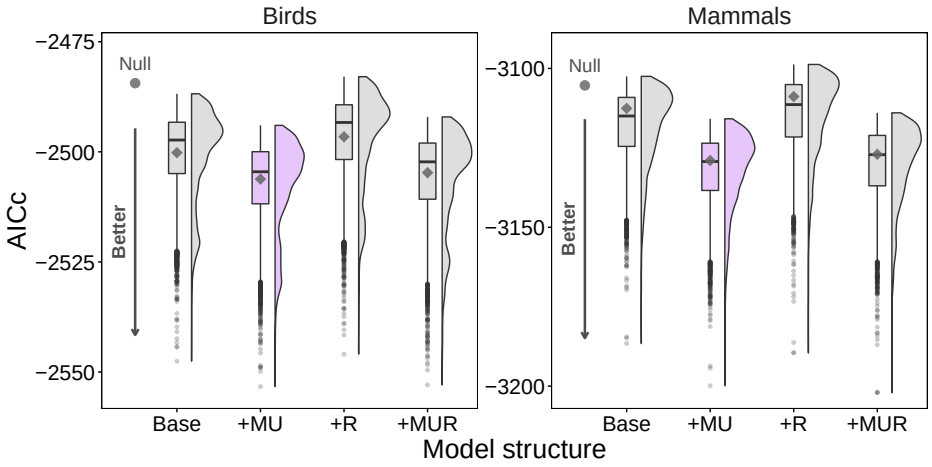

Figure S2.17: **Environmental lags and the inclusion of management and use substantially improve model performance.**
Models incorporating lags (violins and boxplots) can have much better explanatory power (lower AICc) than those without (grey diamonds). Furthermore, models including the management and use status of populations (+MU and +MUR) are better than those that do not.
Boxplots depict the 25%, 50% and 75% quantiles. Whiskers extend 1.5x the interquartile range from the upper/lower quartiles. Points indicate outliers.
Base models incorporate climate change, land-use change (and their interaction), body mass and protected area status as fixed effects. +MU models additionally incorporate management and use status. +R models are as the Base models, but also including realm. +MUR represents models incorporating all of the above variables as fixed effects.

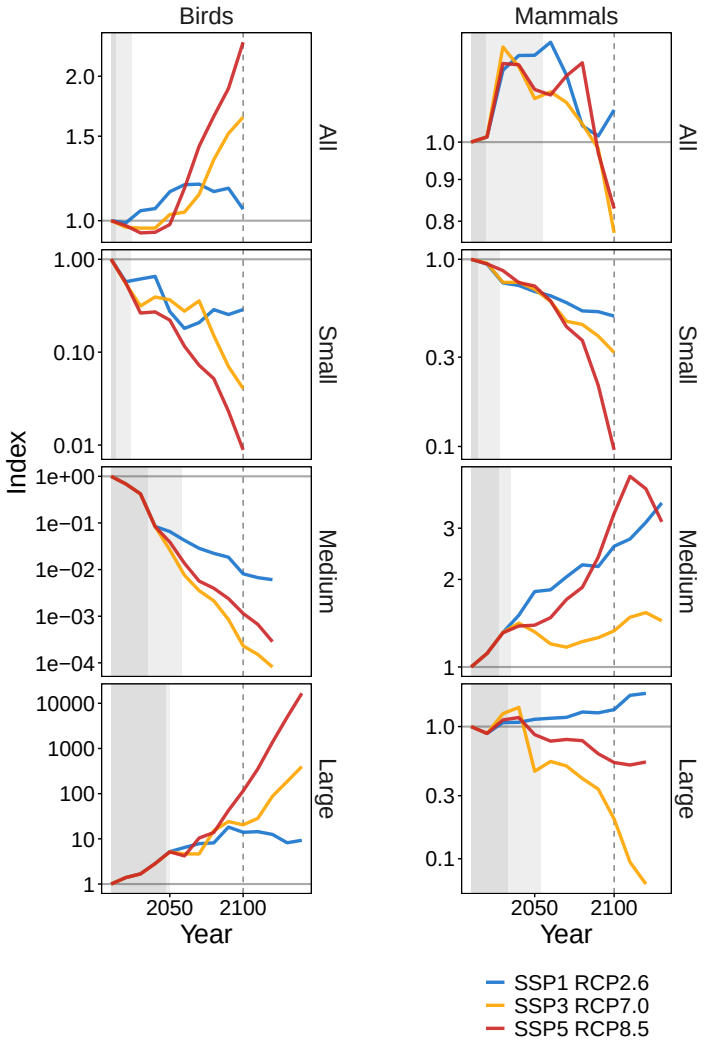

Figure S2.18: **Projections of future abundance indices on independently scaled y-axes.** This figure reproduces the projections presented in our main results, but highlights the variability between scenarios for each vertebrate class and body-size group, whilst also better showing the magnitude of change in each individual panel. Projected abundance indices beyond 2100 (vertical dashed line) are also shown where possible, facilitated by ecological lags.

The horizontal line is set at 1, the baseline for our projections. Shaded areas show future projections that are fully (dark) or partially (light) dependant on environmental change prior to 2010 (in all but medium mammals, climate change is associated with longer lags and thus the lighter shading).

S3 Supplementary tables

Table S3.2: **Summary of the data used in the main analysis.**

Class	Populations	Species	Locations
Aves	830	425	238
Mammalia	921	287	440

Table S3.3: **Definitions of management and use status, as recorded in the Living Planet Database (reproduced and adapted from McRae et al., 2022).**

Data field	Definition	Examples
Used	A population that is intentionally regularly or systematically used, either individuals or eggs. This may be sustainable or unsustainable, and the population does not necessarily have to be threatened by use or over-exploited. This refers to consumptive use whereby individuals or parts of individuals are removed from the wild.	What is included: hunting (including subsistence, sport and trophy hunting); collecting. What is not included: wildlife tourism; education and research in situ; viewing or experiencing for cultural or spiritual reasons.
Managed	A population that receives targeted management (some of which involves sustainable use). This is usually to promote recovery in a population or can incentivise its use for conservation. It can include measures to stem 'unsustainable' population growth.	What is included: supplementary feeding; reintroduction; captive breeding; legal protection; quotas for hunting; provision of nest materials; culling of predators of species being monitored; culling of species being monitored (e.g. if overpopulated). What is not included: protected area (unless it is specifically for that species – e.g. a tiger reserve)

Both fields are coded as 'Yes', 'No' or 'Unknown' and the information is taken from the source of the population data.

Table S3.4: **Summary of the best +MU models (ΔAICc < 6).**

Class	CC lag	LUC lag	Rangeland	AICc	ΔAICc	R^2 (m | c)
Aves	14	3	Incl.	-2553.32	0.00	0.18 | 0.32
	14	2	Incl.	-2549.86	3.46	0.17 | 0.32
	19	3	Incl.	-2549.01	4.31	0.17 | 0.33
	14	1	Incl.	-2548.95	4.37	0.17 | 0.32
	41	2	Incl.	-2548.87	4.45	0.18 | 0.39
	41	3	Incl.	-2548.50	4.82	0.18 | 0.39
	0	0	Incl.	-2506.57	46.74	0.07 | 0.40
	0	0	Excl.	-2505.81	47.51	0.08 | 0.41
Mammalia	45	9	Excl.	-3199.89	0.00	0.14 | 0.42
	45	7	Incl.	-3194.34	5.55	0.14 | 0.44
	0	0	Excl.	-3130.17	69.72	0.07 | 0.39
	0	0	Incl.	-3127.81	72.09	0.06 | 0.40

The best lag-based models display substantially improved explanatory performance (lower AICc and higher marginal R^2) compared to no-lag models.
Models that use no lags are provided for comparison.
Incl. and Excl. indicate whether or not rangeland is considered in the calculation of anthropogenic land cover.
AICc and ΔAICc values are rounded to two decimal places.
In R^2 (m | c), m and c refer to marginal and conditional R^2, respectively.

Table S3.5: **Summary of the best +MUR models (ΔAICc < 6).**

Class	CC lag	LUC lag	Rangeland	AICc	ΔAICc	R^2 (m | c)
Aves	14	3	Incl.	-2552.94	0.00	0.20 | 0.32
	14	2	Incl.	-2549.57	3.37	0.19 | 0.32
	14	1	Incl.	-2548.43	4.52	0.19 | 0.32
	19	3	Incl.	-2547.84	5.11	0.18 | 0.34
	0	0	Incl.	-2505.54	47.40	0.10 | 0.39
	0	0	Excl.	-2503.91	49.03	0.10 | 0.39
Mammalia	45	7	Incl.	-3202.09	0.00	0.15 | 0.43
	45	9	Excl.	-3202.02	0.06	0.15 | 0.42
	45	8	Incl.	-3201.92	0.17	0.15 | 0.43
	0	0	Excl.	-3127.65	74.43	0.07 | 0.39
	0	0	Incl.	-3126.42	75.67	0.07 | 0.40

The best lag-based models display substantially improved explanatory performance (ΔAICc and marginal R^2) compared to no-lag models.
Models that use no lags are provided for comparison.
Incl. and Excl. indicate whether or not rangeland is considered in the calculation of anthropogenic land cover.
AICc and ΔAICc values are rounded to two decimal places.
In R^2 (m | c), m and c refer to marginal and conditional R^2, respectively.

Table S3.6: **Summary of the best models (+MU, ΔAICc < 6) for small species.**

Class	CC lag	LUC lag	Rangeland	AICc	ΔAICc	R^2 (m | c)
Aves	13	3	Incl.	-983.44	0.00	0.18 | 0.64
	13	7	Excl.	-983.13	0.31	0.18 | 0.64
	13	4	Incl.	-982.87	0.58	0.18 | 0.64
	13	1	Incl.	-982.85	0.59	0.18 | 0.63
	13	5	Incl.	-982.39	1.06	0.18 | 0.64
	13	6	Excl.	-982.34	1.11	0.18 | 0.64
	13	2	Incl.	-982.07	1.38	0.18 | 0.64
	13	6	Incl.	-980.96	2.48	0.17 | 0.64
	13	8	Excl.	-980.30	3.15	0.17 | 0.64
	13	7	Incl.	-978.78	4.66	0.17 | 0.63
Mammalia	18	4	Excl.	-1117.23	0.00	0.25 | 0.58
	18	5	Excl.	-1116.30	0.94	0.25 | 0.58
	18	3	Excl.	-1114.71	2.52	0.24 | 0.58
	18	2	Excl.	-1112.22	5.01	0.24 | 0.57

Incl. and Excl. indicate whether or not rangeland is considered in the calculation of anthropogenic land cover.
AICc and ΔAICc values are rounded to two decimal places.
In R^2 (m | c), m and c refer to marginal and conditional R^2, respectively.

Table S3.7: **Summary of the best models (+MU, ΔAICc < 6) for medium species.**

Class	CC lag	LUC lag	Rangeland	AICc	ΔAICc	R^2 (m | c)
Aves	48	25	Excl.	-794.93	0.00	0.25 | 0.39
	48	26	Excl.	-793.88	1.05	0.25 | 0.38
	48	24	Excl.	-791.94	2.99	0.23 | 0.40
	48	27	Excl.	-789.87	5.06	0.24 | 0.38
Mammalia	17	25	Excl.	-1049.52	0.00	0.16 | 0.46
	17	25	Incl.	-1049.10	0.43	0.17 | 0.45
	17	26	Excl.	-1048.82	0.70	0.16 | 0.46
	17	24	Excl.	-1048.14	1.38	0.16 | 0.46
	17	26	Incl.	-1047.70	1.82	0.17 | 0.44
	17	24	Incl.	-1047.06	2.46	0.16 | 0.44
	17	27	Excl.	-1046.98	2.55	0.15 | 0.46
	17	27	Incl.	-1046.62	2.91	0.17 | 0.44
	45	38	Incl.	-1046.16	3.36	0.15 | 0.45
	17	23	Excl.	-1045.69	3.83	0.15 | 0.46
	16	35	Incl.	-1045.51	4.02	0.15 | 0.49
	17	28	Incl.	-1044.86	4.67	0.16 | 0.44
	45	37	Incl.	-1044.81	4.71	0.15 | 0.45
	17	28	Excl.	-1044.47	5.06	0.15 | 0.45
	10	30	Excl.	-1044.17	5.35	0.14 | 0.49
	10	31	Excl.	-1044.15	5.38	0.14 | 0.49
	17	34	Excl.	-1044.12	5.40	0.15 | 0.46
	10	29	Excl.	-1044.02	5.50	0.14 | 0.49
	17	35	Excl.	-1043.95	5.57	0.15 | 0.46
	17	33	Excl.	-1043.95	5.58	0.15 | 0.46
	10	28	Excl.	-1043.64	5.89	0.14 | 0.49
	17	32	Excl.	-1043.59	5.94	0.15 | 0.46
	5	31	Excl.	-1043.54	5.98	0.14 | 0.44

Incl. and Excl. indicate whether or not rangeland is considered in the calculation of anthropogenic land cover.
AICc and ΔAICc values are rounded to two decimal places.
In R^2 (m | c), m and c refer to marginal and conditional R^2, respectively.

Table S3.8: **Summary of the best models (+MU, ΔAICc < 6) for large species.**

Class	CC lag	LUC lag	Rangeland	AICc	ΔAICc	R^2 (m | c)
Aves	40	37	Excl.	-823.18	0.00	0.27 | 0.63
	40	40	Incl.	-822.97	0.20	0.27 | 0.60
	40	39	Incl.	-822.61	0.56	0.27 | 0.59
	40	38	Excl.	-822.58	0.60	0.27 | 0.62
	40	38	Incl.	-822.53	0.65	0.27 | 0.59
	40	41	Incl.	-822.38	0.80	0.27 | 0.60
	40	43	Incl.	-822.35	0.83	0.27 | 0.60
	40	37	Incl.	-822.29	0.89	0.27 | 0.59
	40	42	Incl.	-822.20	0.98	0.26 | 0.60
	40	36	Excl.	-822.18	1.00	0.27 | 0.63
	40	39	Excl.	-821.75	1.43	0.26 | 0.62
	40	40	Excl.	-821.61	1.57	0.26 | 0.62
	40	35	Excl.	-820.99	2.19	0.26 | 0.63
	40	44	Incl.	-820.44	2.74	0.26 | 0.61
	40	41	Excl.	-820.39	2.78	0.26 | 0.62
	40	36	Incl.	-820.14	3.03	0.26 | 0.59
	40	42	Excl.	-819.69	3.49	0.26 | 0.62
	40	3	Excl.	-819.55	3.62	0.26 | 0.50
	40	34	Excl.	-819.33	3.85	0.26 | 0.62
	40	43	Excl.	-819.15	4.03	0.25 | 0.62
	40	33	Excl.	-818.33	4.85	0.26 | 0.61
	40	45	Incl.	-818.15	5.02	0.25 | 0.61
	40	32	Excl.	-818.15	5.03	0.26 | 0.61
	40	35	Incl.	-817.91	5.27	0.26 | 0.59
	40	31	Excl.	-817.56	5.61	0.25 | 0.61
	40	44	Excl.	-817.39	5.79	0.25 | 0.61
Mammalia	44	23	Excl.	-1064.91	0.00	0.22 | 0.49
	44	24	Excl.	-1064.85	0.06	0.22 | 0.49
	44	25	Excl.	-1064.10	0.81	0.22 | 0.50
	19	26	Incl.	-1063.80	1.10	0.22 | 0.48
	44	26	Excl.	-1063.66	1.24	0.21 | 0.50
	19	25	Incl.	-1063.12	1.79	0.21 | 0.48
	44	22	Excl.	-1063.04	1.86	0.22 | 0.49
	44	27	Excl.	-1062.99	1.92	0.21 | 0.49
	44	5	Incl.	-1062.90	2.01	0.24 | 0.52
	19	27	Incl.	-1062.49	2.42	0.21 | 0.48
	22	5	Incl.	-1061.97	2.94	0.22 | 0.49
	44	28	Excl.	-1061.83	3.08	0.21 | 0.49
	44	6	Incl.	-1061.12	3.79	0.24 | 0.52
	44	21	Excl.	-1060.97	3.94	0.22 | 0.49
	16	19	Excl.	-1060.86	4.04	0.24 | 0.53
	19	24	Incl.	-1060.60	4.31	0.21 | 0.48
	19	28	Incl.	-1060.26	4.65	0.21 | 0.48
	16	20	Excl.	-1059.65	5.26	0.24 | 0.52
	44	29	Excl.	-1059.49	5.42	0.20 | 0.49
	13	23	Excl.	-1058.97	5.94	0.23 | 0.43

Incl. and Excl. indicate whether or not rangeland is considered in the calculation of anthropogenic land cover.
AICc and ΔAICc values are rounded to two decimal places.
In R^2 (m | c), m and c refer to marginal and conditional R^2, respectively.

References

Blowes, S. A., Supp, S. R., Antão, L. H., Bates, A., Bruelheide, H., Chase, J. M., ... Dornelas, M. (2019). The geography of biodiversity change in marine and terrestrial assemblages. *Science*, *366*(6463), 339–345.

Burbidge, J. B., Magee, L., & Robb, A. L. (1988). Alternative Transformations to Handle Extreme Values of the Dependent Variable. *Journal of the American Statistical Association*, *83*(401), 123–127.

Côté, I. M., Darling, E. S., & Brown, C. J. (2016). Interactions among ecosystem stressors and their importance in conservation. *Proceedings of the Royal Society B: Biological Sciences*, *283*(1824), 20152592.

ESA. (2017). Land Cover CCI Product User Guide Version 2. Technical Report [Computer software manual]. Retrieved from `maps.elie.ucl.ac.be/CCI/viewer/download/ESACCI-LC-Ph2-PUGv2_2.0.pdf`

Harris, I., Osborn, T. J., Jones, P., & Lister, D. (2020). Version 4 of the CRU TS monthly high-resolution gridded multivariate climate dataset. *Scientific Data*, *7*(1), 1–18.

Hijmans, R. J. (2020). raster: Geographic Data Analysis and Modeling [Computer software manual]. Retrieved from `https://CRAN.R-project.org/package=raster` (R package version 3.4-5)

Hijmans, R. J. (2021). geosphere: Spherical Trigonometry [Computer software manual]. Retrieved from `https://CRAN.R-project.org/package=geosphere` (R package version 1.5-14)

Klein Goldewijk, K., Beusen, A., Doelman, J., & Stehfest, E. (2017). Anthropogenic land use estimates for the holocene – HYDE 3.2. *Earth System Science Data*, *9*(2), 927–953. Retrieved from `https://essd.copernicus.org/articles/9/927/2017/` doi: 10.5194/essd-9-927-2017

Leung, B., Hargreaves, A. L., Greenberg, D. A., McGill, B., Dornelas, M., & Freeman, R. (2020). Clustered versus catastrophic global vertebrate declines. *Nature*, *588*(7837), 267–271.

Lüdecke, D., Ben-Shachar, M. S., Patil, I., Waggoner, P., & Makowski, D. (2021). performance: An R Package for Assessment, Comparison and Testing of Statistical Models. *Journal of Open Source Software*, *6*(60), 3139. doi: 10.21105/joss.03139

McRae, L., Freeman, R., Geldmann, J., Moss, G. B., Kjær-Hansen, L., & Burgess, N. D. (2022). A global indicator of utilized wildlife populations: Regional trends and the impact of management. *One Earth*, *5*(4), 422–433.

Michonneau, F., Brown, J. W., & Winter, D. J. (2016). rotl: an R package to interact with the Open Tree of Life data. *Methods in Ecology and Evolution*, *7*(12), 1476-1481. doi: 10.1111/2041-210X.12593

OpenTreeOfLife, Redelings, B., Reyes, L. L. S., Cranston, K. A., Allman, J., Holder, M. T., & McTavish, E. J. (2019). *Open Tree of Life Synthetic Tree.* Zenodo. Retrieved from `https://doi.org/10.5281/zenodo.3937741` doi: 10.5281/zenodo.3937741

Paradis, E., & Schliep, K. (2019). ape 5.0: an environment for modern phylogenetics and evolutionary analyses in R. *Bioinformatics*, *35*, 526-528.

Piggott, J. J., Townsend, C. R., & Matthaei, C. D. (2015). Reconceptualizing synergism and antagonism among multiple stressors. *Ecology and Evolution*, *5*(7), 1538–1547.

Revell, L. J. (2012). phytools: An r package for phylogenetic comparative biology (and other things). *Methods in Ecology and Evolution*, *3*, 217-223.

Spooner, F. E., Pearson, R. G., & Freeman, R. (2018). Rapid warming is associated with population decline among terrestrial birds and mammals globally. *Global Change Biology*, *24*(10), 4521–4531.

Williams, J. J., Freeman, R., Spooner, F., & Newbold, T. (2021). Vertebrate population trends are influenced by interactions between land use, climatic position, habitat loss and climate change. *Global Change Biology*.